Supplementary Material

1 Supplementary Tables

Table S1. Classifications of droughts by SPEI

Grade	SPEI	Type
1	≥2.00	Extreme wet
2	1.50~1.99	Severe wet
3	1.00~1.49	Moderate wet
4	0.50~0.99	Mild wet
5	-0.50~0.49	Normal
6	-1.00~-0.51	Mild drought
7	-1.50~-1.01	Moderate drought
8	-2.00~-1.51	Severe drought
9	≤-2.00	Extreme drought

Table S2. Descriptions of meteorological data

Name	Units	Description
RH	%	This parameter is the percentage of water vapor pressure in air saturation value (the point at which water vapor begins to condense into liquid water or deposit into ice). For temperatures above 0 °C (273.15 K), calculate the saturation of the effluent. Calculate the saturation on the ice at temperatures below - 23 °C. Between - 23 °C and 0 °C, this parameter is calculated by interpolating between ice and water values using a quadratic function.
V10/U10	m·s-1	The northward/easterly component of this parameter is the horizontal velocity at which the air moves north/East. A minus sign indicates that the air moves south/West.
SST	K	This parameter (SST) is the sea water temperature near the surface. In ERA5, this parameter is the basic SST, which means that there is no change due to the daily cycle of the sun (diurnal variation).
TA	K	HadCRUT5 is a global temperature data set, which provides global grid temperature anomalies and average temperature anomalies in the hemisphere and the whole earth. This paper uses the average temperature anomaly in the northern hemisphere.

Table S3. Description of large-scale climate indices

Name	Description
EP-NP	The East Pacific - North Pacific (EP- NP) pattern is a Spring-Summer-Fall pattern with three main anomaly centers. The positive phase of this pattern features positive height anomalies located over Alaska/ Western Canada, and negative anomalies over the central North Pacific and eastern North America.
SOI	The SOI is defined as the normalized pressure difference between Tahiti and Darwin, which reflects the activity of El Nino. The correlation is that if the SOI has a persistent negative value, there would be an El Nino phenomenon this year. .
AMO	It is the SST anomaly occurring in the North Atlantic region with a basin scale and a 10-year variability. It is a natural variability with a period of 65 ~ 80 A and an amplitude of 0.4 ℃.

Table S4. Features of Top 10 major drought events

Rank	Longitude (°)	Latitude (°)	Duration (m)	Severity	Starting Month(m-a)	Peak Month(m-a)	Ending Month(m-a)	Clustering Region
1	-70.75	9.25	42	-95.09	Apr-13	Jun-14	Oct-16	1
2	35.75	16.25	39	-82.04	Jun-08	Jun-09	Sep-11	7
3	72.75	19.75	31	-103.81	Sep-15	Nov-17	May-18	7
4	46.75	10.75	31	-99.92	Sep-13	Aug-15	Apr-16	1
5	43.75	34.25	31	-91.26	Jan-98	Nov-98	Sep-00	1
6	-142.25	64.25	33	-78.46	Aug-92	Jul-93	May-95	5
7	47.75	10.75	30	-107.38	Nov-72	Dec-74	May-75	1
8	71.25	21.25	30	-84.21	Oct-78	Apr-80	May-81	7
9	-143.75	64.75	31	-77.64	Sep-92	Mar-93	May-95	4
10	-109.25	27.75	33	-68.4	Jan-95	May-96	Oct-97	7

Note: Negative longitude indicates west longitude and positive longitude indicates east longitude; A positive value of latitude indicates north latitude; The unit of duration is the total number of months; The unit of the first and last months is the year, which is represented by numbers in the cluster area$R_i (i = 1, \ldots, 7)$.

2 Supplementary Figures

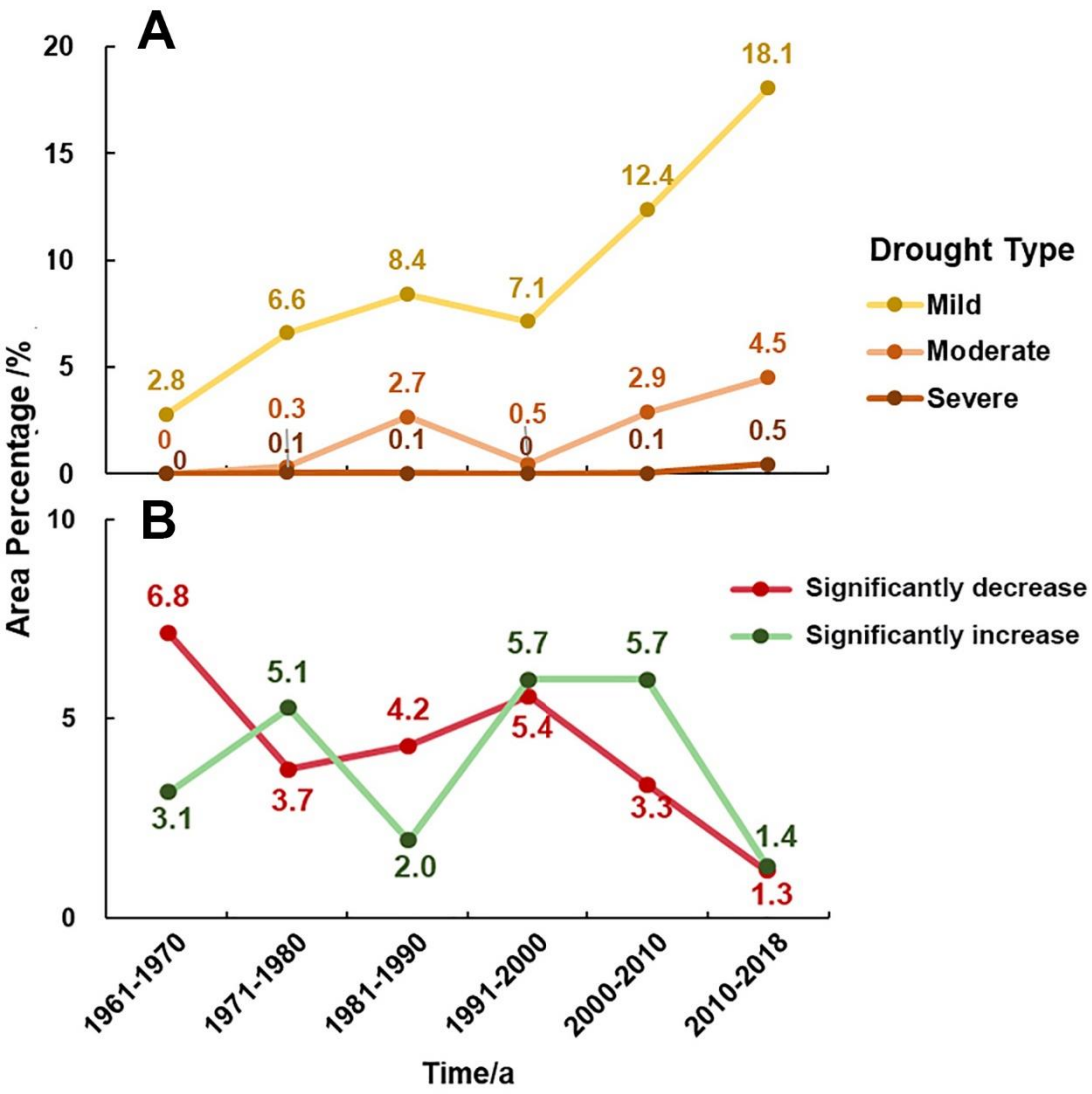

Figure S1. Percentage of drought-affected regions based on SPEI. (A) Percentage of drought-affected regions by mild, moderate and severe droughts. (B) Percentage of regions dominated by droughts with significant increasing and/decreasing trends using MMK technique.

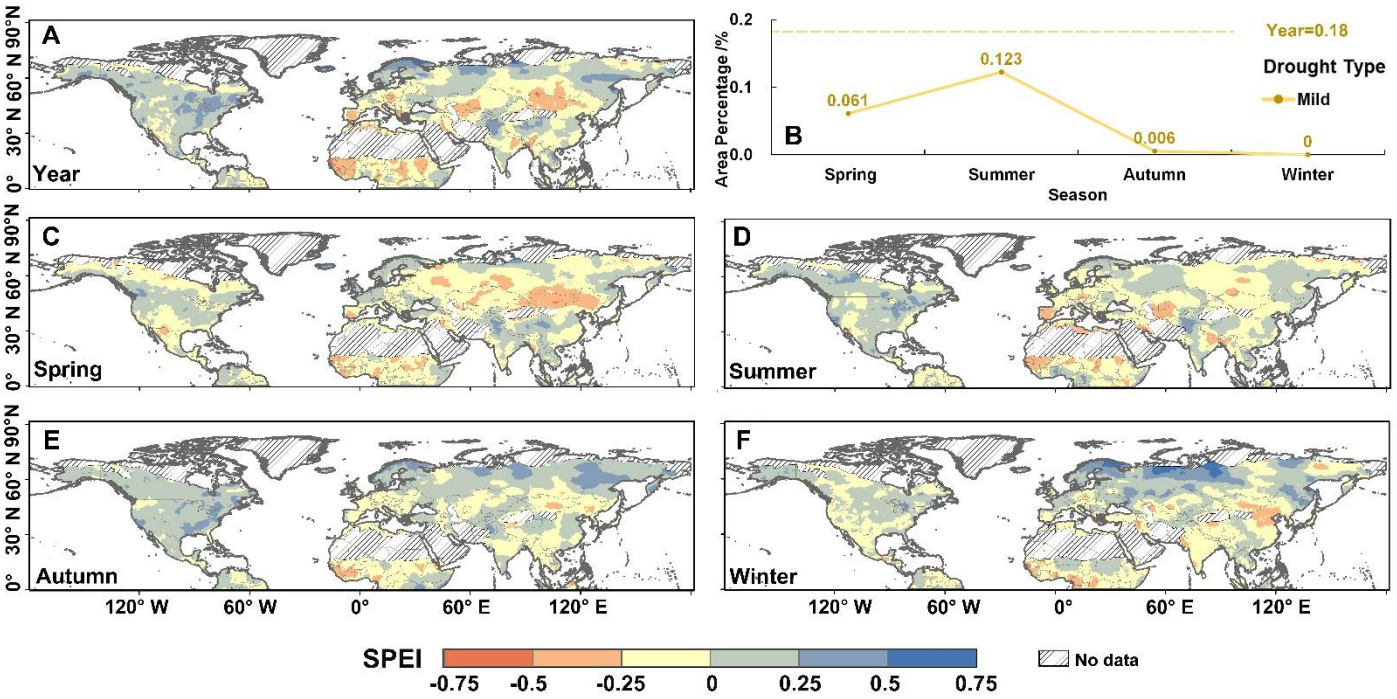

Figure S2. Spatiotemporal evolutions of SPEI at annual and seasonal scales from 1961 to 2018. (A) at annual scale; (B) percentage of drought affected regions at annual and seasonal scales; (C-F) at seasonal scales: (C) in spring; (D) in summer; (E) in autumn; (F) in winter.

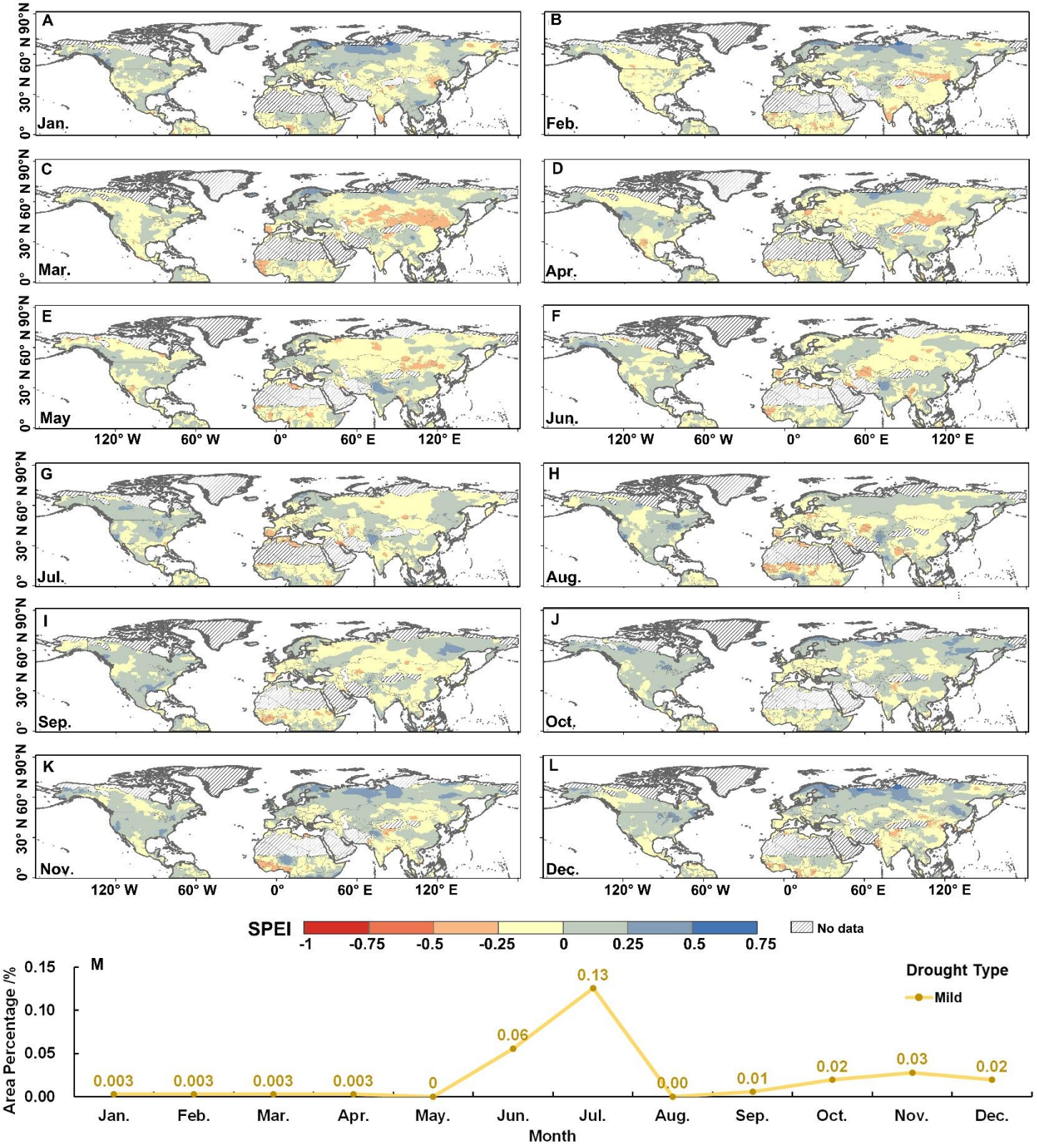

Figure S3. Spatiotemporal evolution of SPEI at monthly scale from 1961 to 2018. (A) in January; (B) in February; (C) in March; (D) in April; (E) in May; (F) in June; (G) in July; (H) in August; (I) in September; (J) in October; (K) in November; (L)in December; (M) percentage of drought affected regions at monthly scales.

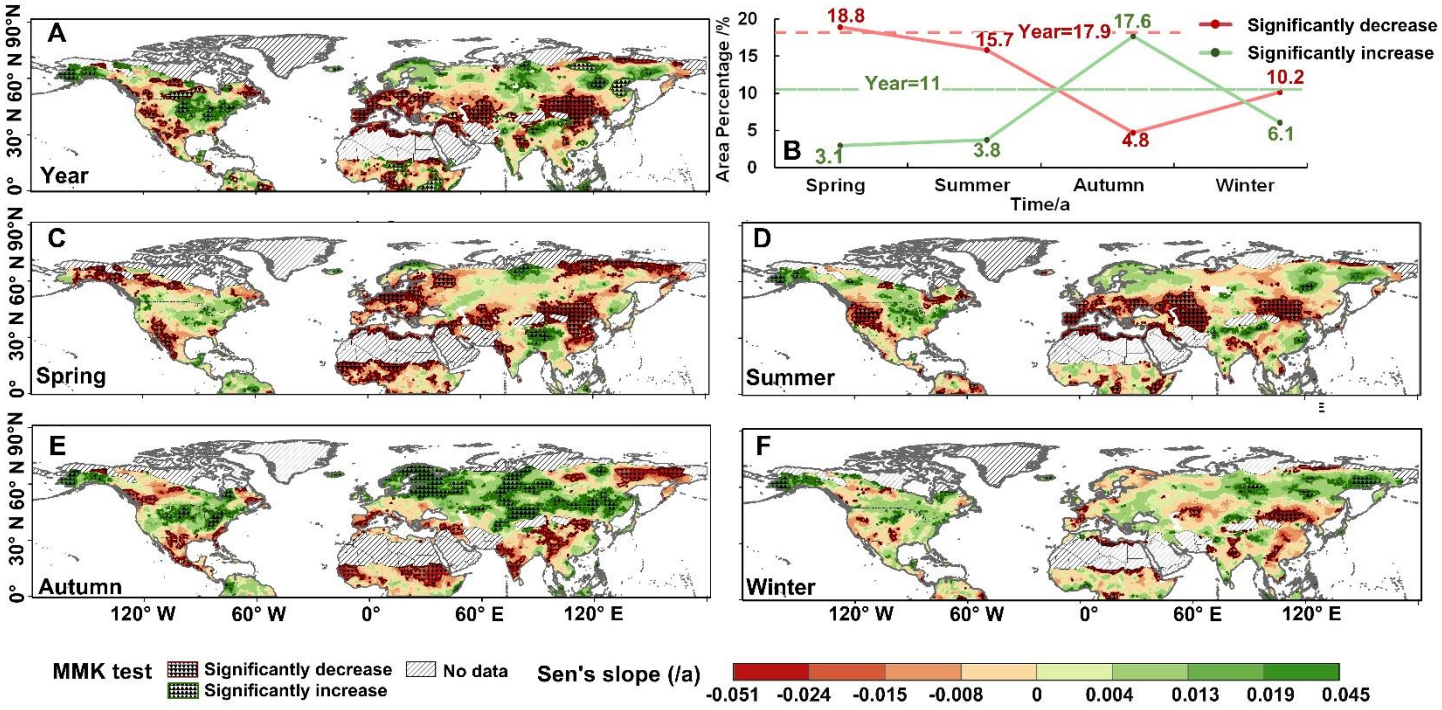

Figure S4. Spatiotemporal evolution of trends in SPEI at annual and seasonal scales from 1961 to 2018 based on MMK trend and Sen's slope methods. (A) at annual scale; (B) percentage of drought affected regions at annual and seasonal scales; (C-F) at seasonal scales: (C) in spring; (D) in summer; (E) in autumn; (F) in winter.

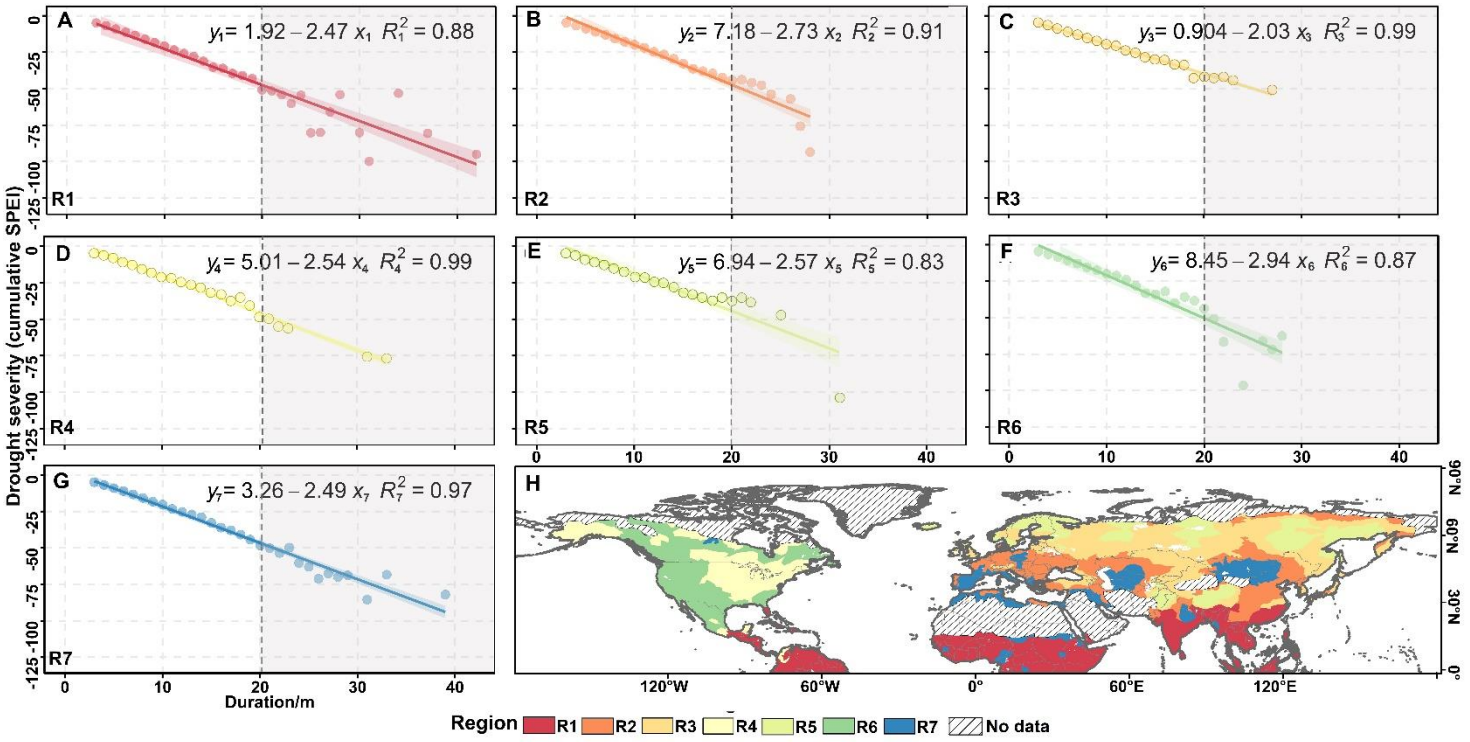

Figure S5. Relationship between drought duration and drought severity for each subregion. (A) R1; (B) R2; (C) R3: (D) R4; (E) R5; (F) R6; (G) R7; (H) Spatial pattern of subregions.

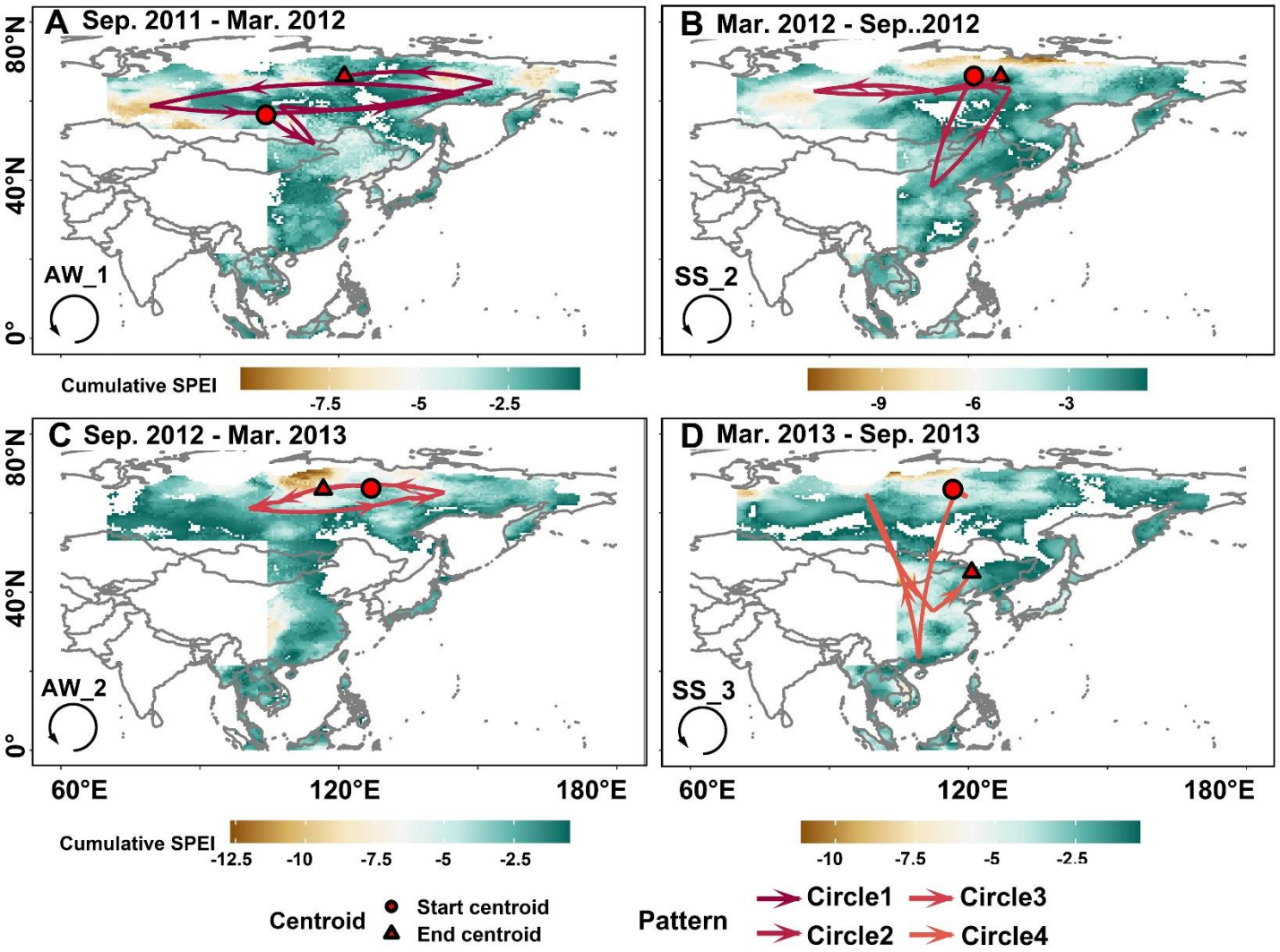

Figure S6. Drought migration trajectories in NES from September 2011 to September 2013. (A) September 2011 - March 2012; (B) March 2012- September 2012; (C) September 2012 - March 2013; (D) March 2013 - September 2013.

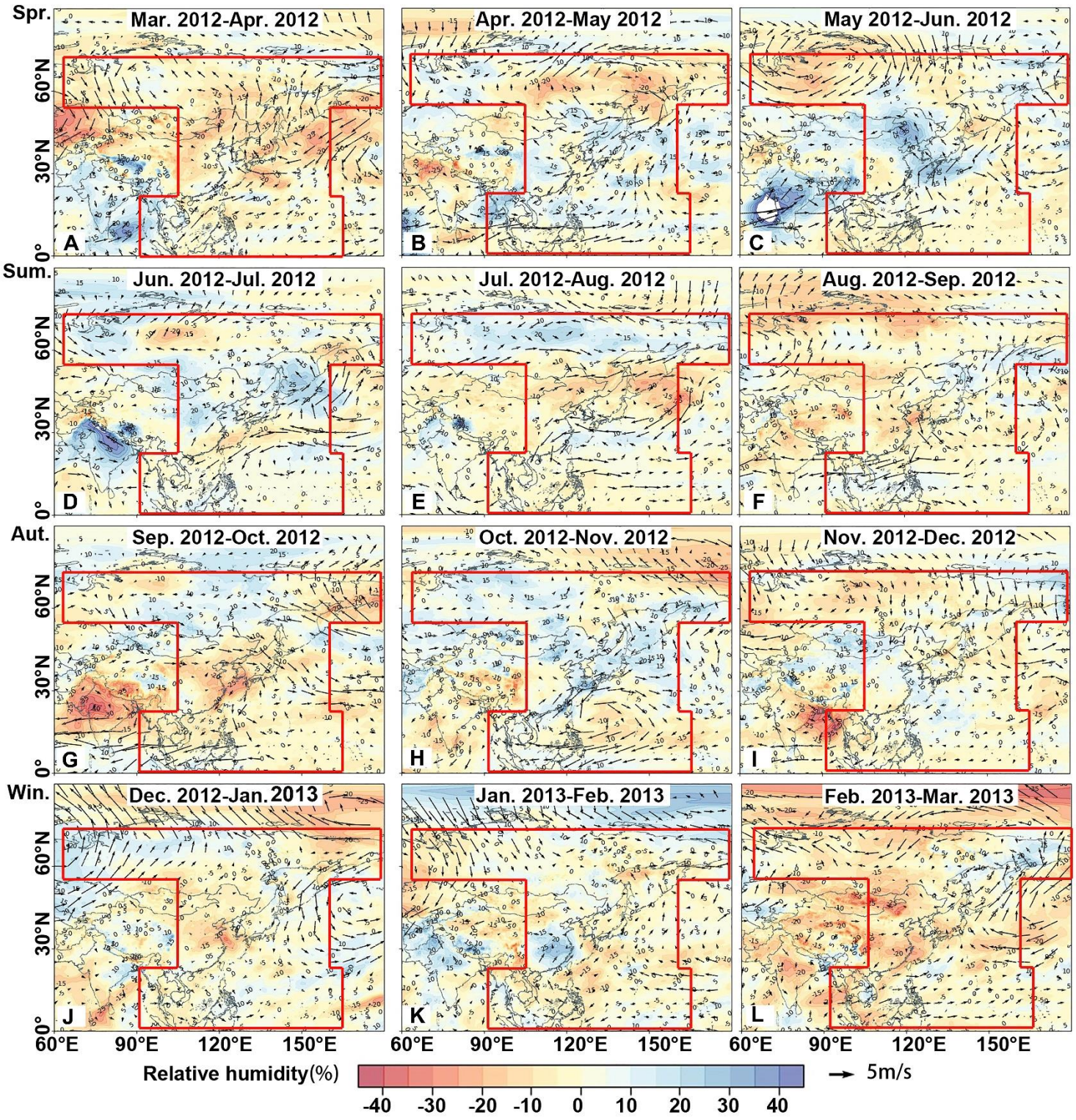

Figure S7. Water vapor variations in NES from March 2011 to March 2012. (A) March 2012- April 2012; (B) April 2012 - May 2012; (C) May 2012 - June 2012; (D) June 2012 - July 2012; (E) July 2012 - August 2012; (F) August 2012 - September 2012; (G) September 2012 - October 2012; (H) October 2012 - November 2012; (I) November 2012 - December 2012; (J) December 2012 - January 2013; (K) January 2013 - February 2013; (L) February 2013 - March 2013. The red box refers to the boundary of NES.

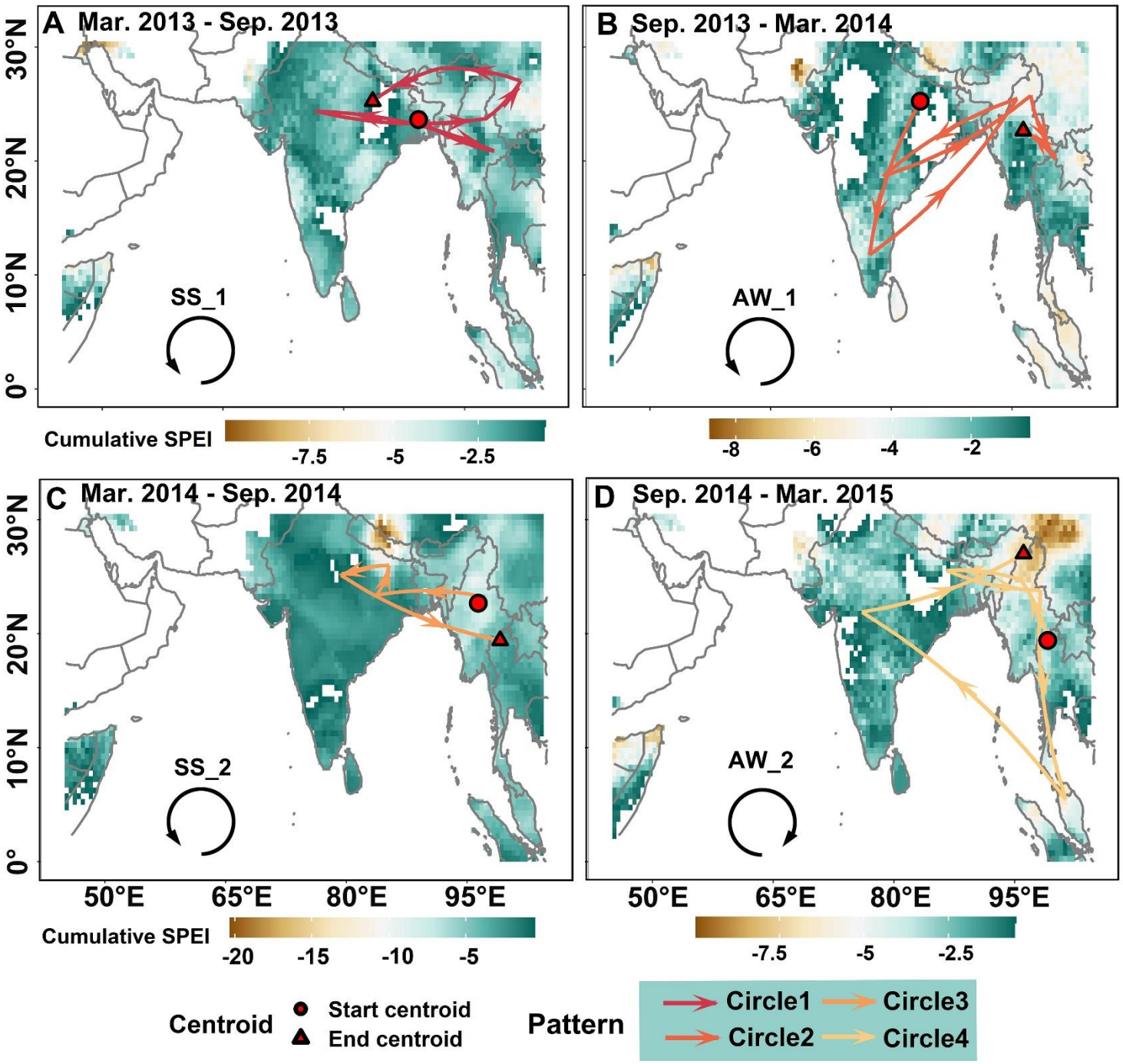

Figure S8. Drought migration trajectories in SAS from March 2013 to March 2015. (A) March 2013 - September 2013; (B) September 2013 - March 2014; (C) March 2014 - September 2014; (D) September 2014 - March 2015.

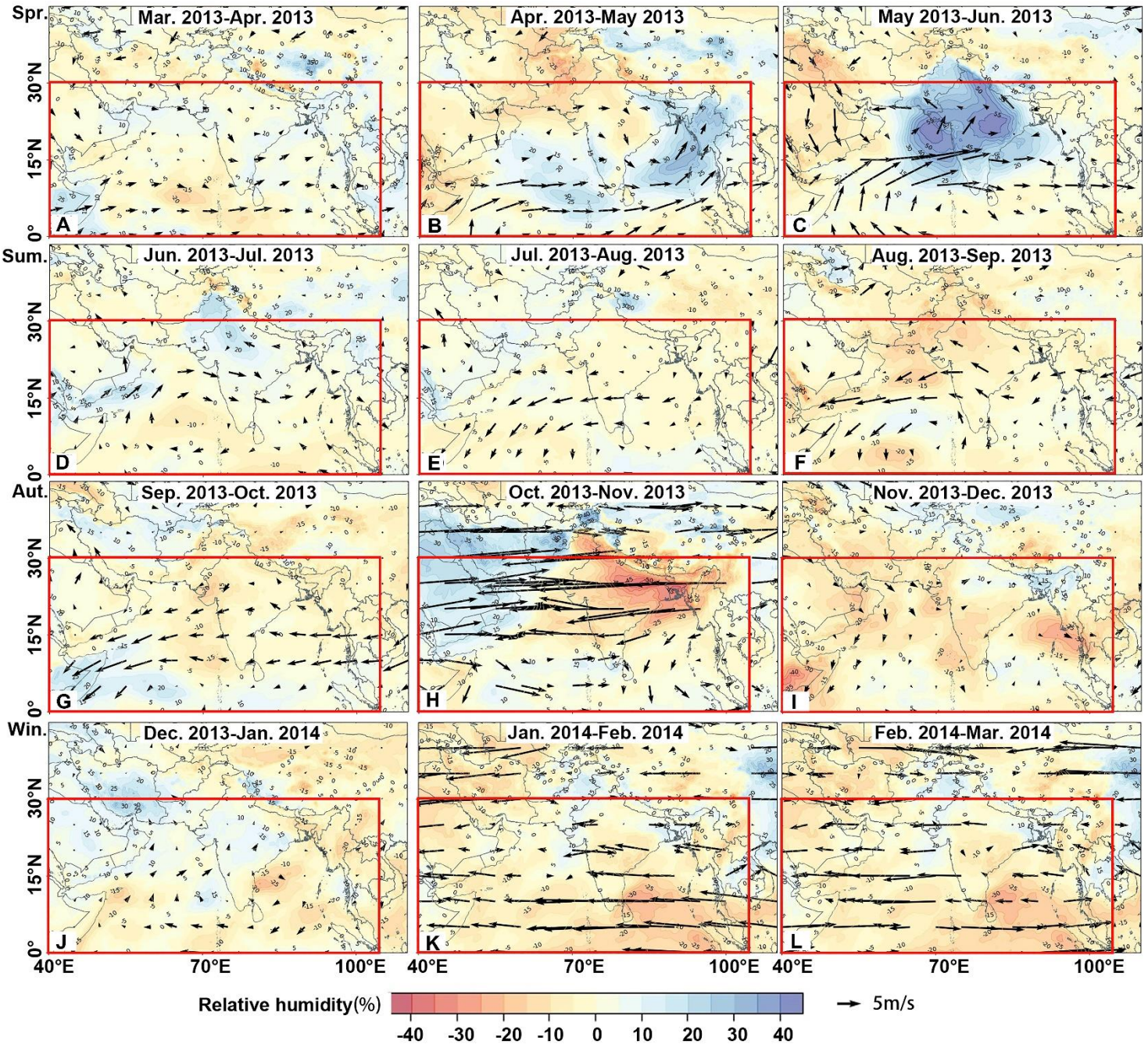

Figure S9. Water vapor variations in SAS from March 2013 to March 2014. (A) March 2013 - April 2013; (B) April 2013 - May 2013; (C) May 2013 - June 2013; (D) June 2013 - July 2013; (E) July 2013 - August 2013; (F) August 2013 - September 2013; (G) September 2013 - October 2013; (H) October 2013 - November 2013; (I) November 2013 - December 2013; (J) December 2013 - January 2014; (K) January 2014 - February 2014; (L) February 2014 - March 2014. The red box refers to the boundary of SAS.

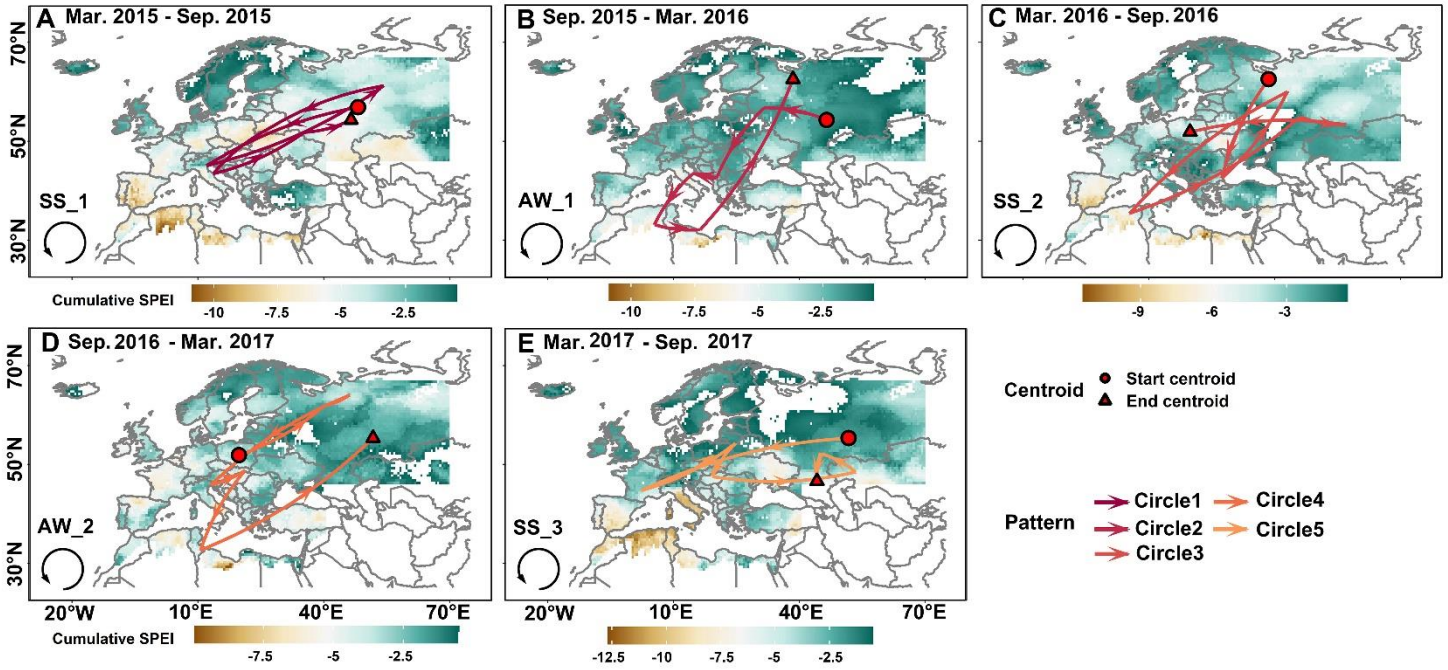

Figure S10. Drought migration trajectories in EU from March 2015 to September 2017. (A) March 2015 - September 2015; (B) September 2015 - March 2016; (C) March 2016 - September 2016; (D) September 2016 - March 2017; (E) March 2017 – September 2017.

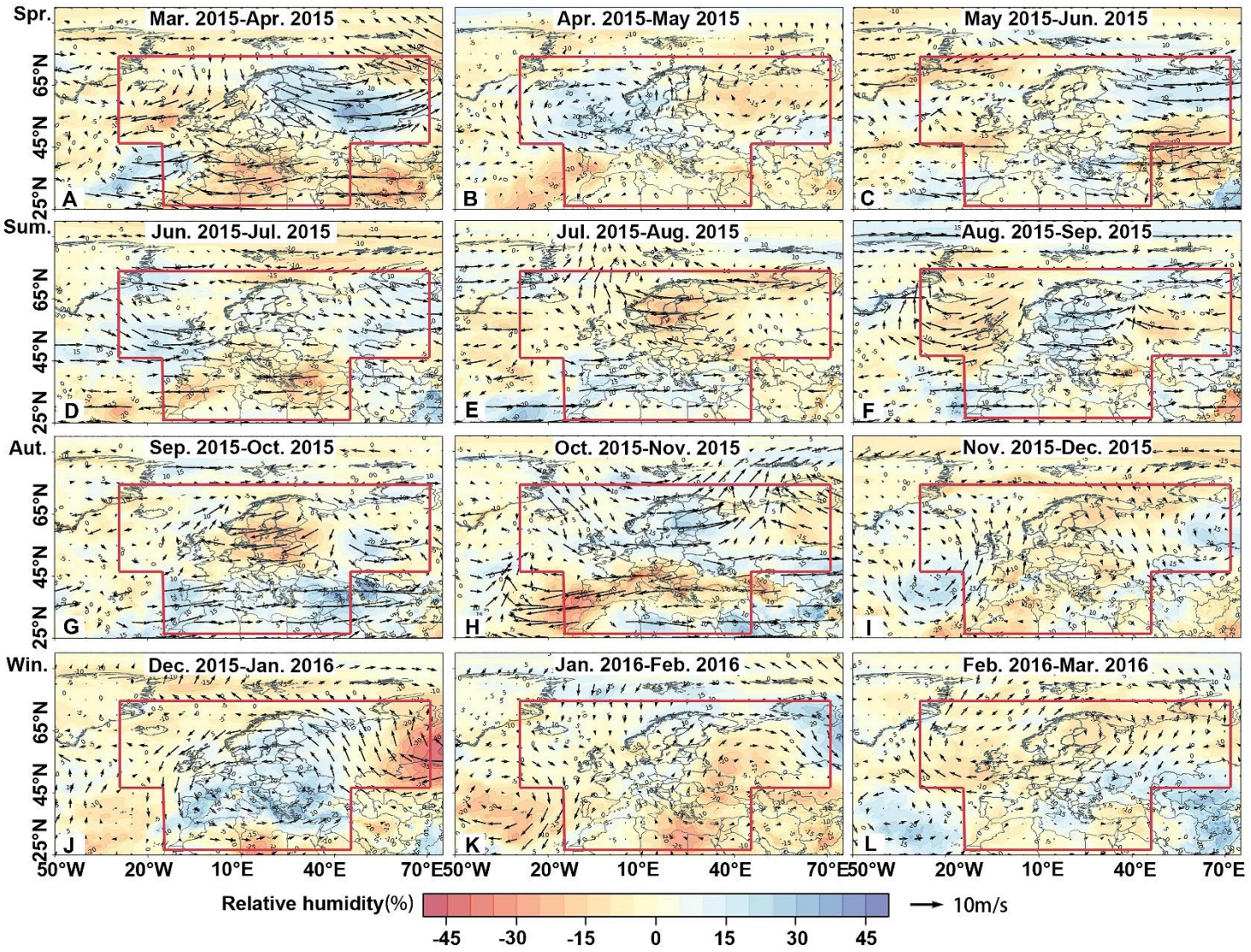

Figure S11. Water vapor variations in EU from March 2015 to March 2016. (A) March 2015 - April 2015; (B) April 2015 - May 2015; (C) May 2015 - June 2015; (D) June 2015 - July 2015; (E) July 2015 - August 2015; (F) August 2015 - September 2015; (G) September 2015 - October 2015; (H) October 2015 - November 2015; (I) November 2015 - December 2015; (J) December 2015 - January 2016; (K) January 2016 - February 2016; (L) February 2016 - March 2016. The red box refers to the boundary of EU.

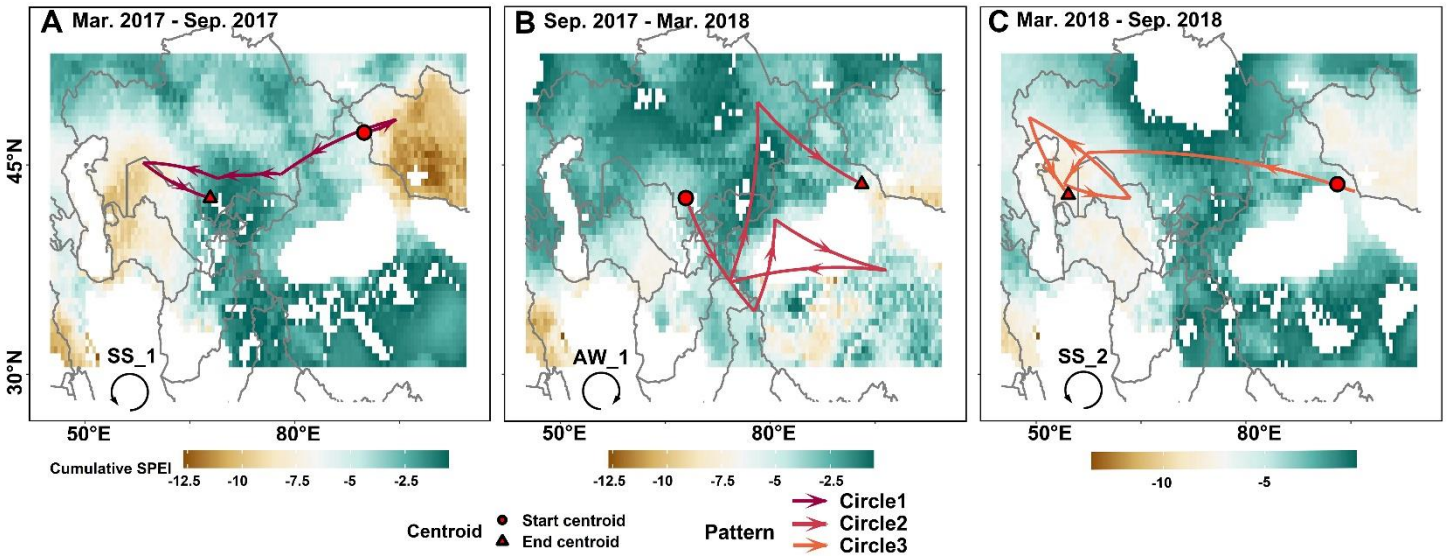

Figure S12. Drought migration trajectories in CT from March 2017 to September 2018. (A) March 2017 - September 2017; (B) September 2017 - March 2018; (C) March 2018 - September 2018.

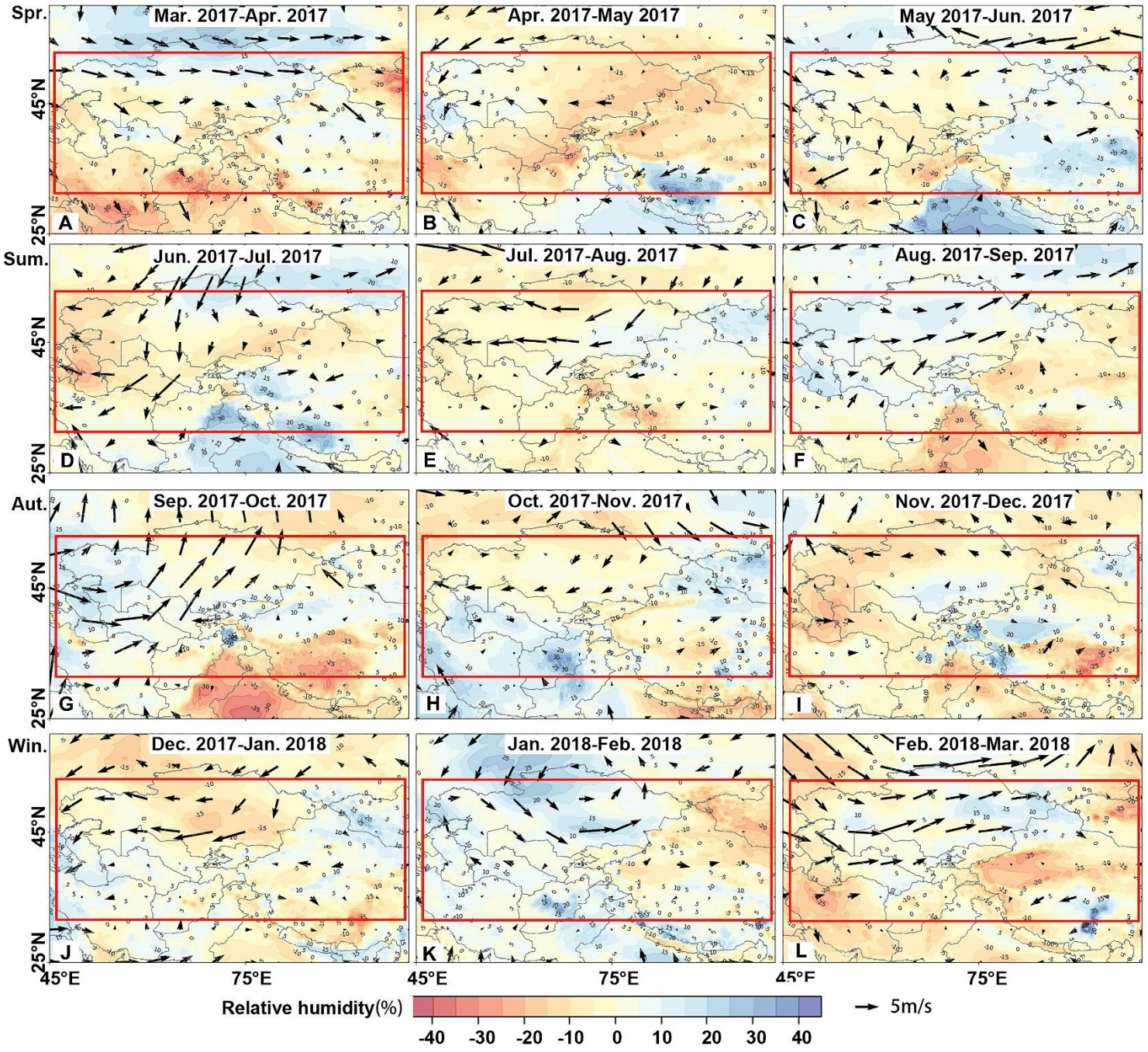

Figure S13. Water vapor variation in CT from March 2017 to March 2018. (A) March 2017 - April 2017; (B) April 2017 - May 2017; (C) May 2017 - June 2017; (D) June 2017 - July 2017; (E) July 2017 - August 2017; (F) August 2017 - September 2017; (G) September 2017 - October 2017; (H) October 2017 - November 2017; (I) November 2017 - December 2017; (J) December 2017 - January 2018; (K) January 2018 - February 2018; (L) February 2018 - March 2018. The red box refers to the boundary of EU.